

## Simulation Model of a Three-Phase Grid-Connected PV Generation System under Various Loading Conditions

Subiyanto<sup>1</sup>, Djoko Adi Widodo<sup>2</sup>

Department Electrical Engineering  
Semarang State University  
50229 Semarang, Indonesia

<sup>1</sup>(biyantote\_unnes@yahoo.com)

<sup>2</sup>(dawte\_unnes@yahoo.com)

---

**Abstract**—This paper presents a simulation modeling and for a three phase grid-connected photovoltaic system using MATLAB SIMULINK. The simulation uses parameter from the available data of Sanyo HIP-200BA3 module. Twenty five modules are utilized in order to build a 4 kW PV system. The system mainly consists of a PV panel, a DC-DC boost converter for maximum power point tracking controller, three phase inverter, point common coupling of the grid and loads. The control system is developed in the MATLAB/Simulink to track maximum power of PV operation and the inverter. It generates a pulse-width modulation signals for switching devices (IGBTs) with the accomplishment of fuzzy logic controller and Park transformation. The performance of the PV system when connected to the static or dynamic loads is investigated in terms of maximum power tracking and load increase. Performance of the inverter is capable of generating the 50 Hz sinusoidal ac output current with total harmonic distortion of 0.06 % which is below its harmonic limit of 5 %. The results show that the total maximum power of the PV system is 4 kW and the system gives good load following performance when subjected to increase in static and dynamic loads. More results such as voltages, current and system power flow are presented to validate the efficacy of the simulation model.

**Keywords** —photovoltaic, grid connected, fuzzy logic, MPPT, 3-phase inverter

---

### I. INTRODUCTION

Nowadays, global surface temperatures have increased because of the global warming taking place due to effluent gas emissions and increase in carbon dioxide (CO<sub>2</sub>) in atmosphere which contributes to greenhouse effect [1]. Other problems with energy supply and use are related not only to global warming but also to environmental concerns such as pollution, acid precipitation, ozone depletion, forest destruction, and radioactive substance emissions but also related depletion of conventional energy resources. To minimize these effects, some potential solutions have evolved including energy conservation through improved energy efficiency, a reduction in fossil fuel use and an increase in renewable energy supplies. Renewable energy sources are considered as a technological option for generating clean, efficient and environmentally-friendly sources as to significantly contribute to the sustainable energy supply. Photovoltaic (PV) generation system is one of the promising renewable energy technologies [1, 2]. It is considered as a clean and environmentally-friendly source of energy. However, the widespread use of PV systems poses several challenges such as increasing the efficiency of energy conversion, fluctuating output power which varies with temperature, irradiation and partial shading, ensuring the reliability of power electronic converters and meeting the requirements for grid connection [3]. PV modules have unique current vs voltage (I-V) characteristics. From the I-V characteristics, PV systems must be operated at a maximum power point (MPP) of specific current and voltage values so as to increase the PV efficiency. For any PV system, the output power can be increased by tracking the MPP of the PV module by using a controller connected to a boost converter [4]. However, the MPP changes with irradiation level and temperature due to the nonlinear characteristic of PV modules [5]. Each type of PV module has its own specific characteristic and this makes the tracking of MPP a complicated problem. To overcome this problem, many maximum power point tracking (MPPT) control algorithms have been presented. Fuzzy logic has been used for tracking the MPP of PV modules because it has the advantages of being robust, relatively simple to design and does not require the knowledge of an exact model [6].

In this paper, a boost converter is modeled for MPPT media beside as for step-up DC voltage to meet the needs of a 3-phase inverter input and a 3-phase inverter is also modeled to ensure stable PV power fed to the grid.

As for the control algorithm developed for both the MPPT controller and inverter, fuzzy logic is applied. In the fuzzy logic based MPPT algorithm, the linguistic variables for FLC are derived from the traditional perturbation and observation method. Implementation of the fuzzy logic based MPPT algorithm is first simulated in MATLAB/Simulink. A modification is made to the fuzzy logic presented in [7] in terms of fuzzification and rule base.

Many research works have been carried out on grid connected PV systems focusing on the development of various technologies and control strategies. In this paper, a dynamic simulation model of a grid connected PV system is presented by using MATLAB SIMULINK. The dynamic model of PV system is derived based on a set of mathematical equation and subsystems. The objective of the study is to investigate the performance of the grid connected PV system when connected to both static and dynamic loads by using load increase as a contingency. Different load characteristic may give different response to the PV system. Simulations are carried out by connecting the grid connected PV system to the different types of loads which are subjected to various loading conditions.

## II. MODEL OF GRID CONNECTED PV SYSTEM

The proposed scheme of grid connected PV generation system is shown in Fig. 1. The system consists of a grid, a photovoltaic array to generate electric power, dc-dc controller with MPPT, dc-ac inverter, transformer and static or dynamic load. The modeling details of these sub systems are presented next.

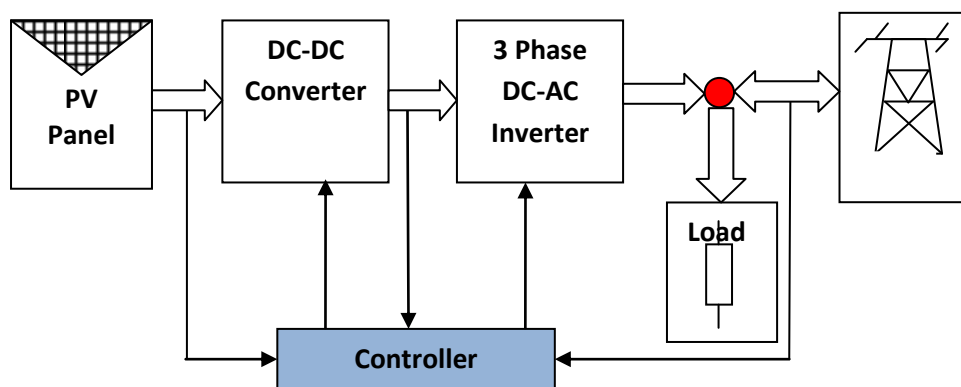


Fig 1 Schematic diagram of a transformer-less 3 phase grid connected PV system

### II.1. PV Array Model

A typical model of a solar cell can be represented by an ideal current source, a diode ( $D$ ) to represent the p-n semiconductor junction, internal series resistance ( $R_s$ ) and internal shunt resistance ( $R_{sh}$ ) as shown in Fig. 2 [8]. Generally, the value of  $R_{sh}$  is very large and the value of  $R_s$  is very small and can be neglected to simplify the analysis. The series resistance should be as low as possible and its shunt resistance should be very high, so that most of the available current can be delivered to the load. The photo current,  $I_{ph}$  represents the cell photocurrent (current source) generated by photovoltaic effect. The output voltage (cell voltage),  $V_{Cell}$  and the cell current,  $I_{Cell}$  of the solar cell supply power to the load depending on the ambient temperature and the sun irradiation.

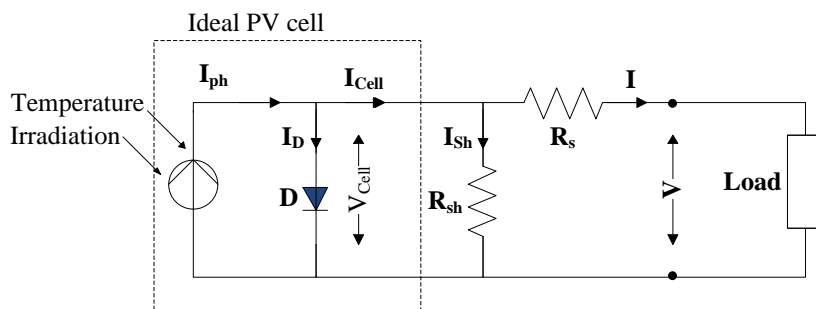


Fig 2 Equivalent circuit of a solar cell

The current at the p-n junction of the PV cell is represented by the diode equation given as,

$$I_D = I_{Sat} \left( e^{\left( \frac{qV}{a \cdot k_B T} \right)} - 1 \right) \quad (1)$$

The saturation current of a diode ( $I_{Sat}$ ) depend on the material semiconductor. It is play an importance role of a PV cell performance. Considering an ideal PV cell where the series resistance,  $R_S$  and parallel resistance,  $R_{Sh}$  are neglected, the PV cell current is given by,

$$I = I_{cell} = I_{load} = I_{ph} - I_D \quad (2)$$

$$I = I_{ph} - I_{Sat} \left( e^{\left( \frac{qV}{a \cdot k_B T} \right)} - 1 \right) \quad (3)$$

Knowing that  $V = V_{Cell}$  and considering the behaviour of a real solar cell, the two parasitic resistances inside the cell, namely,  $R_S$  and  $R_{Sh}$  are taken into account and the PV cell current becomes,

$$I = I_{cell} = I_{load} = I_{ph} - I_D - I_{Sh} \quad (4)$$

$$I = I_{ph} - I_{Sat} \left( e^{\left( \frac{q(V_{Cell} + I_{Cell} R_S)}{a \cdot k_B T} \right)} - 1 \right) - \frac{V_{Cell} + I_{Cell} \cdot R_S}{R_{Sh}} \quad (5)$$

where,

- $V$  : terminal voltage of the PV cell (V)
- $V_D$  : voltage across P-N junction diode
- $V_{Cell}$  : ideal PV cell voltage
- $I$  : PV cell current (A)
- $I_D$  : diode current ( $p-n$ )(A)
- $R_S$  : series resistance (Ohm)
- $I_{ph}$  : photo current (A)
- $T$  : Temperature (K)
- $a$  : diode ideal constant
- $I_{Sat}$  : saturation current of the p-n junction (A)
- $q$  : charge of an electron  $1.6 \times 10^{-19}$  Coulomb
- $k_B$  : Boltzmann constant,  $1.38 \times 10^{-23}$  J/K

## II.2. Boost Converter Circuit

A boost converter is a DC to DC power converter with output voltage always greater than the input voltage [9]. Fig. 3 shows a boost converter, consisting of DC input voltage source  $V_{in}$ , boost inductor  $L$ , controlled switch  $S$ , diode  $D$ , output filter capacitor  $C$ , and load  $R_L$ . During switch  $S$  is closed ( $0 < t < t_{on}$ ) and switch  $S$  is opened ( $t_{on} < t < T_S$ ) the equivalent circuits are depicted in Fig. 3.

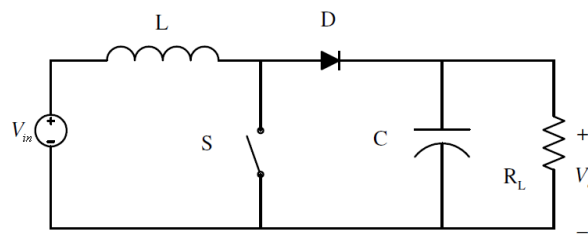


Fig 3 A simple boost converter circuit

The current continuously flows in the inductor, the time integral of the inductor voltage must be zero over one switching period ( $T_S$ ) [9].

$$V_{in} t_{on} + (V_{in} - V_o) t_{off} = 0 \quad (6)$$

The voltage gain ( $Gi$ ) is derived from (2.19) as follows:

$$Gi = \frac{V_o}{V_{in}} = \frac{T_S}{t_{off}} = \frac{1}{1-d} \quad (7)$$

in which the duty cycle ratio,  $d$  is a fraction of time during the switch on.

$$d = \frac{t_{on}}{T_s} \quad (8)$$

### II.3. Inverter

There are three topologies in the PV inverters applications, namely central inverter, string inverter, and integrated inverter [10]. In this research, a central inverter topology is used. This topology is used due to low cost topology.

Inverter topologies can be basically divided two types namely, the current source inverter (CSI) and voltage-source inverter (VSI) [11]. In this research an inverter model directly connected to the PV module uses single-stage power conversion system for feed-in using CSI type as shown in Fig 4[11].

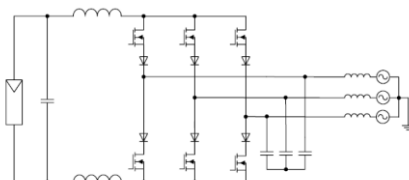


Fig 4 Scheme of three phase CSI for a PV module generation system inverter.

Consider the fundamental frequency component of the rms line-to-line output voltage of a three phase inverter which varies with the DC input voltage and modulation ratio. Its mathematical relationship is given by [9]:

$$V_{LL,rms} \approx 0.612 \cdot m_a \cdot V_d \quad (9)$$

where,

$V_{LL,rms}$  : rms line-to-line output voltage of the 3 phase inverter

$m_a$  : modulation ratio ( $0 < m_a < 1$ )

$V_d$  : DC input voltage of the 3 phase inverter

### II.4. Load

The load models are traditionally classified into two broad categories namely, static and dynamic models. The static load model expresses the characteristics of the load at any instant of time as algebraic functions of the bus voltage magnitude and frequency at that instant. The active power component (P) and reactive power component (Q) are considered separately. Traditionally, the voltage dependency of load characteristics has been represented by exponential model as follows.

$$P = P_o (\bar{V})^{n_p} \quad (10)$$

$$Q = Q_o (\bar{V})^{n_q} \quad (11)$$

$$\bar{V} = \left( \frac{V}{V_o} \right) \quad (12)$$

where,

$P_o$  : initial active power

$Q_o$  : initial reactive

$V$  : instantaneous voltage

$V_o$  : initial voltage

$n_p$  : slope  $dP/dV$  at  $V=V_o$

$n_q$  : slope  $dQ/dV$  at  $V=V_o$

Dynamic load is a type of load that changes in the direction or degree of force during operation. The three-phase dynamic load is modeled as three-wire dynamic load whose P and Q varies as a function of positive-sequence voltage. The three load currents are considered balance. The dynamic model is expressed as follows

$$P_{(s)} = P_o \left( \frac{V}{V_o} \right)^{n_p} \frac{(1 + T_{p1} s)}{(1 + T_{p2} s)} \quad (13)$$

$$Q_{(s)} = Q_o \left( \frac{V}{V_o} \right)^{n_p} \frac{(1 + T_{q1} s)}{(1 + T_{q2} s)} \quad (14)$$

where

- Tp1, Tp2 : time constants to control the dynamics of the active power P.  
 Tq1, Tq2 : time constants to control the dynamics of the reactive power Q.

### III. METHODOLOGY

In the proposed method, the PV module considered in the simulation is Sanyo HIP-200BA3 with a capacity of 4 kW. Initially the grid connected PV is considered to be connected with static load which has capacity of 20 kW + j4 kVAR (above PV capacity) and 2 kW + j1 kVAR (below PV capacity). The power will be recorded from the grid and PV system to determine how much power is contributing from both sources. To determine the performance of the system during dynamic load, initially a single static load with a capacity of 2 kW + j1 kVAR is connected to the system. The load is then increased in steps of 10 kW + j2 kVAR, to investigate the performance of the PV when connected to the static load. This step is then repeated by using the dynamic load. The voltage-current (V-I) characteristic of the PV system is determined from the simulation. The maximum power of PV system is also investigated by tracking the output current and voltage of each PV module. Fig.5 shows the simulation model of a grid-connected PV system implemented in MATLAB.

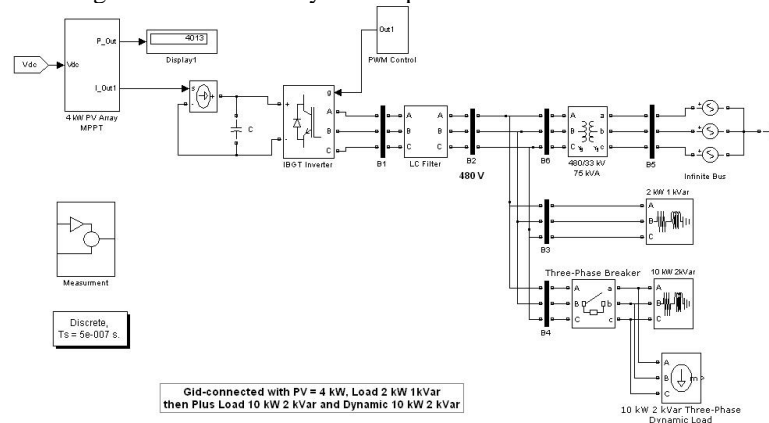


Fig 5 Modeling of dynamic grid connected PV system in MATLAB.

To illustrate the effectiveness of the proposed dynamic grid connected PV model, a simple two bus system is studied. The required data for solar module is shown in Table 1.

Table 1. Data of solar module

Product	Sanyo
Seri Model	HIP-200BA3
Rated power	200 W
Efficiency of cell	19.7 %
Vmp	55.8 V
Imp	3.9 A
Voc	68.7 V
Isc	3.83 A
$\alpha$ :current temperature coefficients	0.88
$\beta$ :voltage temperature coefficients	-0.172

For this simulation, the number of PV modules is 20 modules of solar panel to build PV array. The configuration of PV array is shown in Fig. 6.

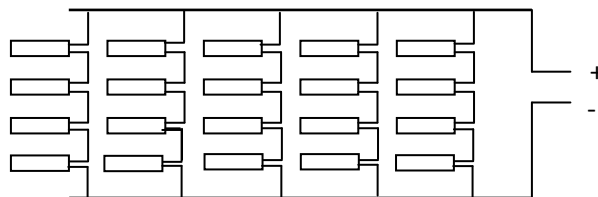


Fig 6 The configuration of Sanyo Solar (PV) modules to build a 4 kW PV generation system.

In this simulation, the subsystem block which considers the DC-DC converter with MPPT and characteristic of the PV module are shown in Figs. 7(a) and 6(b), respectively.

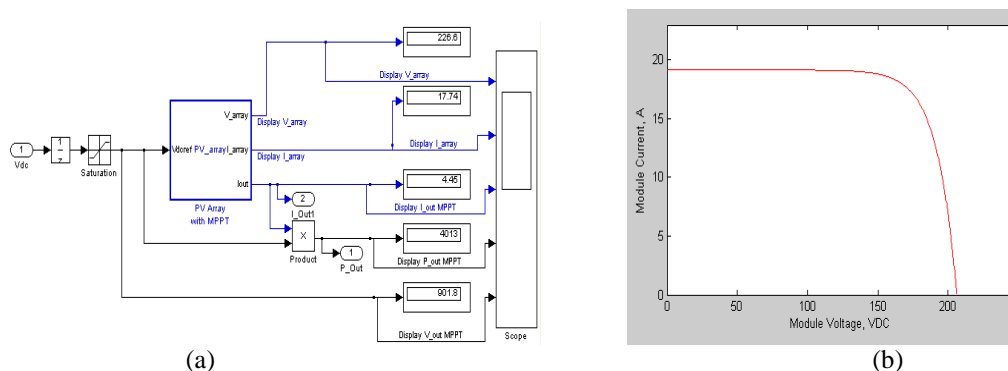


Fig 7 (a) DC-DC converter with MPPT in the PV system (b) Characteristic of PV module.

To model the PV module, the short circuit current ( $I_{sc}$ ) and the open circuit voltage ( $V_{oc}$ ) must be considered. From Table 1,  $I_{sc}$  is 3.83 A, and  $V_{oc}$  is 68.7 volt. Hence at the design voltage and current can be in the range of 0 to 68.7 volt and 0 to 3.83 A, respectively.

The main components in fuzzy logic based MPPT controller are fuzzification, rule-base, inference and defuzzification as shown in Fig. 8. The input variables to the controller are the change in PV array power ( $\Delta P_{pv}$ ) and change in current ( $\Delta I_{pv}$ ) whereas the output of the controller is the step change of boost converter current reference ( $\Delta I_{ref}$ ). The current reference is the current that must be drawn from the PV array to the boost converter.

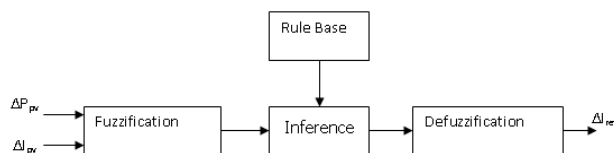


Fig 8 Main components in fuzzy logic.

Fig. 9 shows the control strategy of the grid-connected inverter. The control algorithm mainly comprises of voltage and current control, PWM signal generation, grid disturbance detection and system protection. In the voltage control, the dc input voltage,  $V_{dc}$  is regulated by the FLC which generates the current reference,  $I_{dref}$  to be tracked by the controllers in the current control loop.

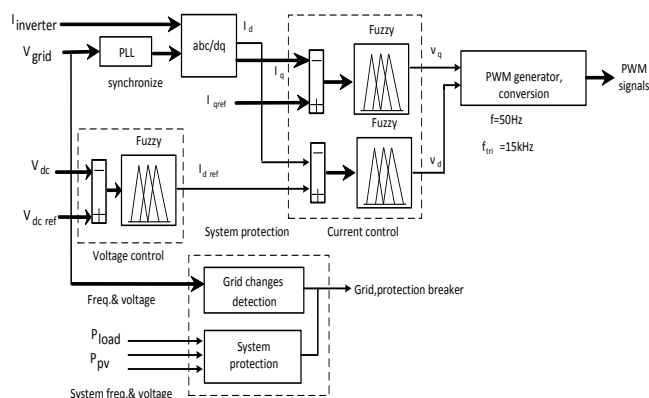


Fig 9 Fuzzy logic based inverter control strategy

The maximum power can be calculated by multiplying the output current with output voltage that can give maximum power. Based on maximum voltage at each module which is 56.65 volt, the voltage of PV array is  $56.6500 \times 4 = 226.6000$  volt. Besides, the maximum current drawn by each PV which is found to be 3.5481 amp and therefore the total current of the PV array is 17.740 amperes ( $3.5481 \times 5$ ). The MPP of each PV can be calculated from maximum output voltage and maximum output current which is equal to 200.6520 watt.

The maximum power that can be obtained from 20 modules of PV array is 4013.04 watt which is almost similar to the simulated PV array of 4kW. Fig. 10 (a) shows the profile of MPPT of the PV module.

To calculate the profile of output current of the DC/DC converter, rated voltage of the inverter must be considered. The reference input voltage to inverter is 900 V, so the output DC-DC converter must be set to 900 V. Since maximum power from PV array is 4013.04 Watt and assuming that there are no losses in DC-DC converter, the output current of the converter can be calculated as  $I_{out} = 4013.04/900 = 4.459$  A. The output current profile of the converter is shown in Fig. 10(b).

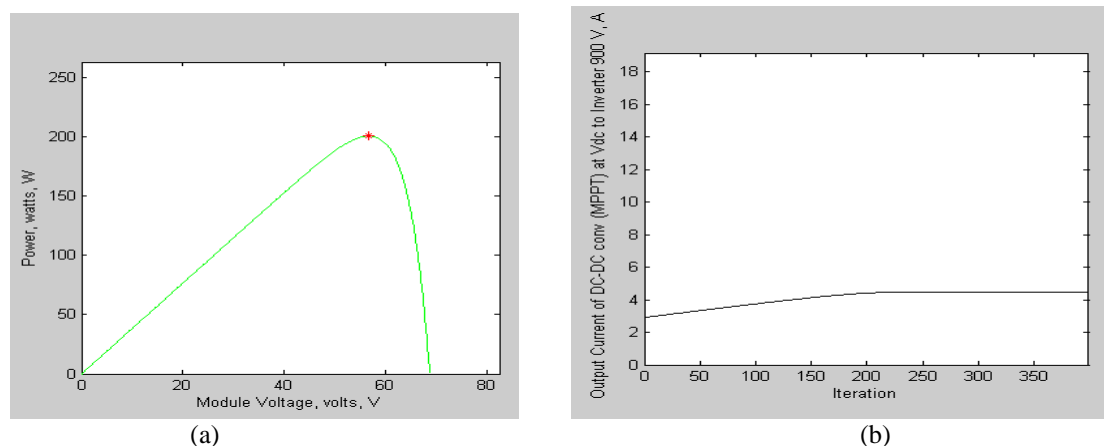


Fig 10 (a) Tracking of maximum power point, (b) output current of DC-DC converter.

#### IV. RESULT AND DISCUSSION

##### IV.1. Result from grid connected PV system analysis

In this section, power profiles of PV during loading for fixed operating conditions are presented. Figs. 11 - 14 shows the profile of P and Q of the load from power flow direction. Two scenarios is used in the study, firstly amount of load is considered to be within capacity of PV system and secondly the load is assumed to be greater than the rated capacity of PV system.

From Figs.11 (a) and (b) shows the power profile when system is connected to the load 2 kW + j1 kVAR, the PV system fully supply to the load and the rest of the available capacity from PV system is transferred to the grid system (positive P and Q) as shown in Figs. 11(a)-(b). In this case The maximum power that can be obtained from 20 modules of PV array is 4013.04 watt which is almost similar to the simulated PV array of 4 kW. PV system

is directly connected to grid without any battery installed. If the battery installed, than the power will be transferred to charge the battery.

In the other hand, when the load connected is greater than PV capacity such as  $20 \text{ kW} + j 4 \text{ kVAR}$  as shown in Figs. 12(a)-(b). In this case the PV system fully utilized supply to the load (4 kW) and the rest (16 kW + j4 kVAR) coming from the grid. Negative sign of P and Q means that the system received power from the grid.

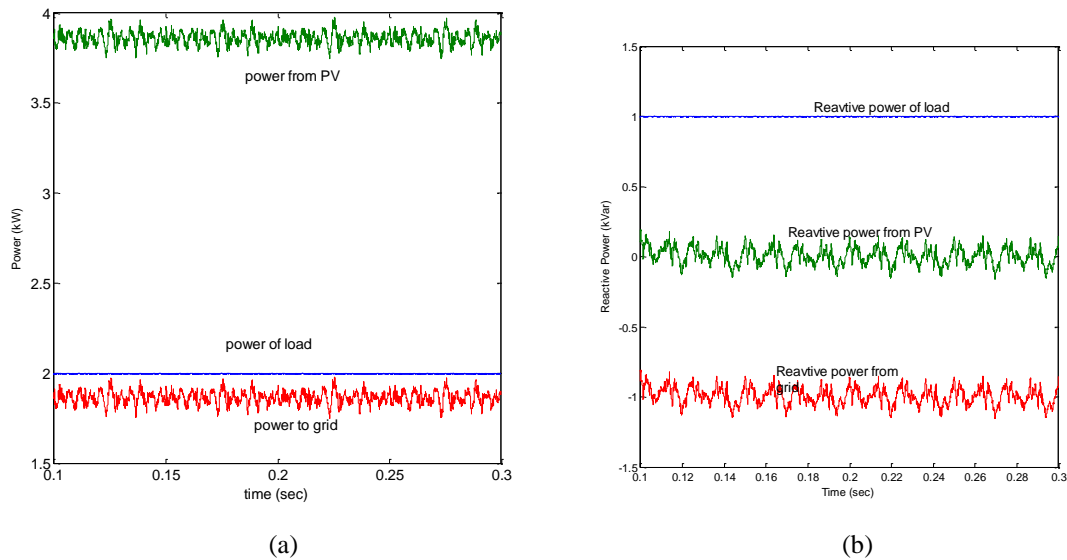


Fig 11 (a) Active power profile (b) Reactive power profile when load power is lower than PV capacity.

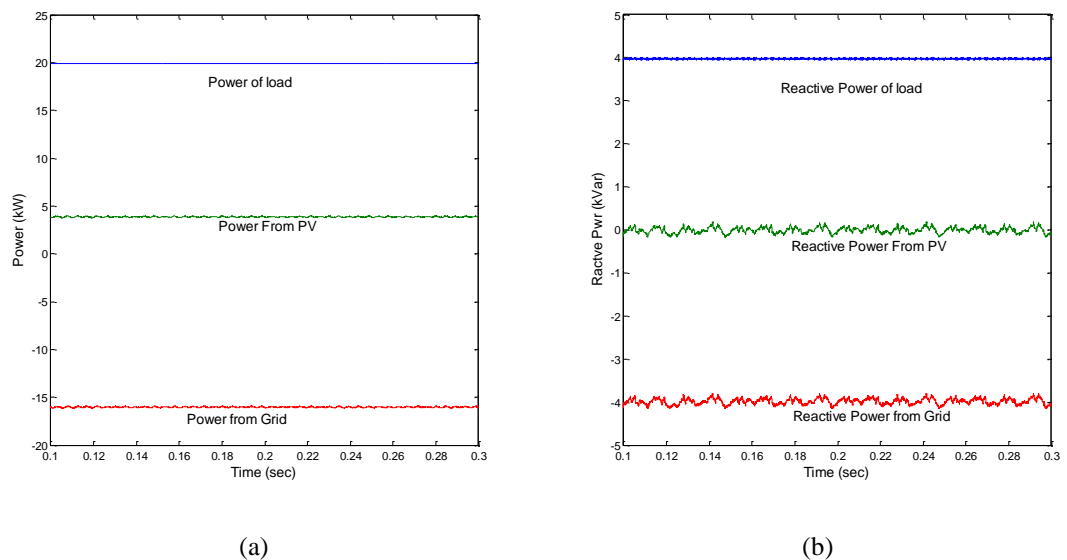


Fig 12 (a) Active power profile (b) Reactive power profile when load power is greater than PV capacity.

#### IV.2. Result Due to Change in the Load

The performance of the grid connected PV during load increase contingency is described on Figs. 13 and 14. Figs. 13(a) and (b) shows addition of static load and Figs. 14(a) and (b) illustrates increment of dynamic load which is connected between time  $t=0.17 \text{ sec}$  and  $0.34 \text{ sec}$ .

From Figs.13 (a)-(b) it can be seen that the power due to static load increase and decrease. Before additional load, the load is below maximum capacity of PV system. Since the PV system always supply constant power the rest of power flows into the grid. It can be seen from the power grid is positive. After the load increase, power to the grid is becoming negative. It means the grid starts to supply power to the load. Supply power from PV still remains constant.



The characteristic due to load increase and decrease also investigated for dynamic load. The result will be showed at Figs. 14(a)-(b). It can be seen from Figs. 14 that dynamic load increase is more effect to the system rather than increasing static load. System loading increases due to reactive power absorb from the load but it can cover lost power from the grid supply. The performances of PV have l little effect on load variations. It can be seen that the overall performance of the PV system is very good (always constant at maximum power).

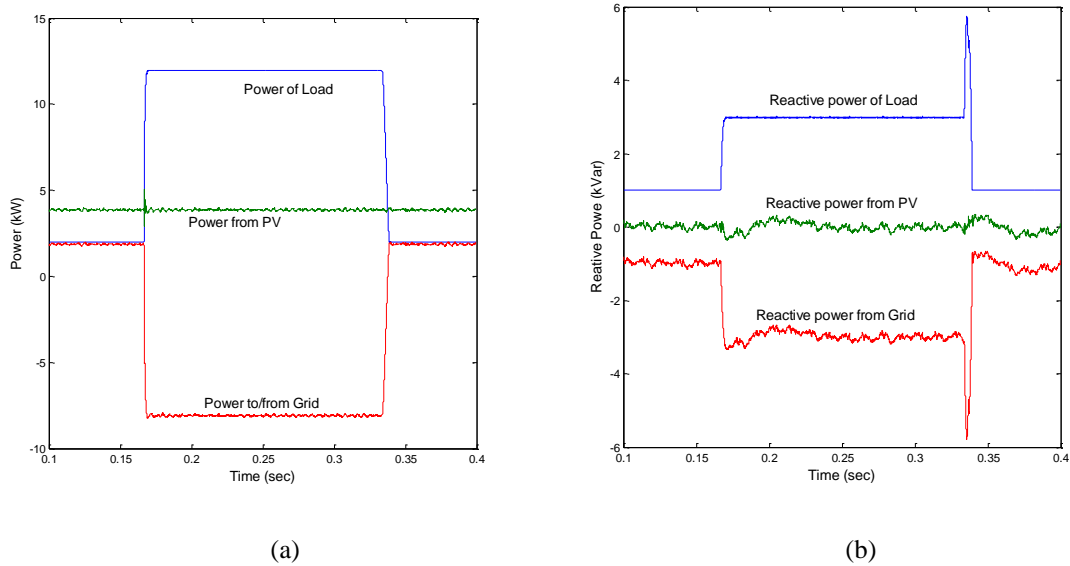


Fig 13 (a) P profile (b) Q profile due to static load increase.

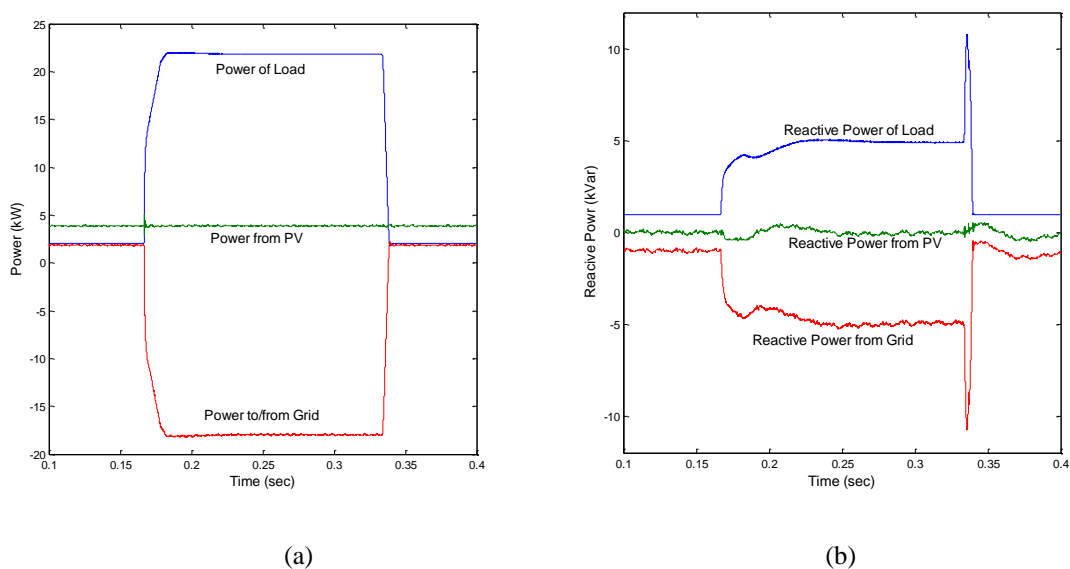


Fig 14 (a) P profile (b) Q profile due to dynamic load increase

To investigate the output voltage quality of the inverter, a Fast Fourier Transform (FFT) analysis has been performed. In the analysis, the total harmonic distortion (THD) at the point of common coupling which is the point between the inverter and the grid was computed and the harmonics frequency spectrum was obtained as depicted in Fig. 15. From the FFT analysis, it is seen that the THD of the inverter output voltage is 0.06%. It is well lower to the standard THD limit of 5% (IEEE standard) [12].

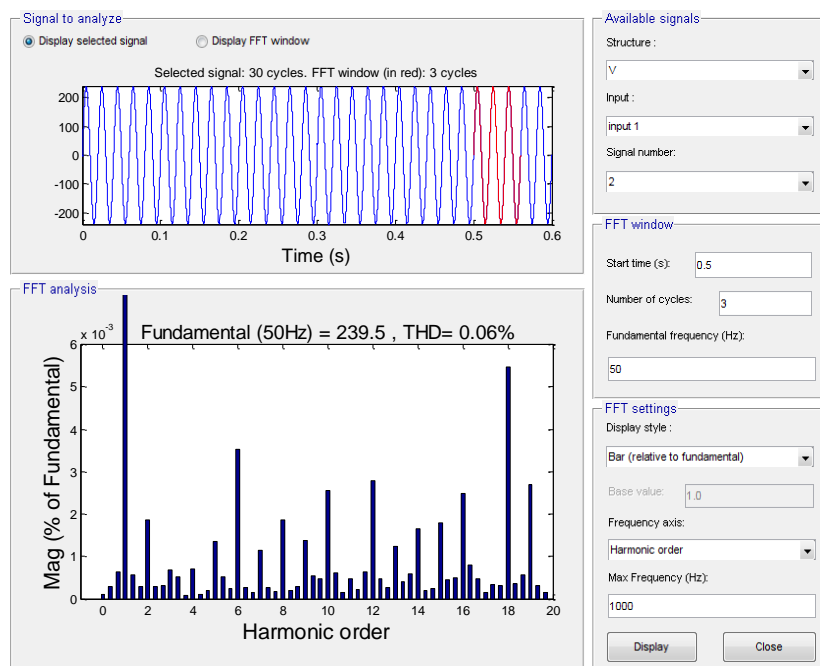


Fig 15 THD and harmonic spectrum of the phase A inverter output voltage

## V. CONCLUSION

Modeling and simulating grid connected dynamic PV systems are important to realize good design of PV system that can be connected to the grid. In this paper, dynamic grid connected PV 4 kW system is modeled and simulated by using the data from a practical model of 20 Sanyo solar modules HIP-200BA3. A dynamic and static load increase variation is used to observe the characteristic of the grid connected PV system. From the simulation results, it is shown that the maximum power from PV array that can be obtained is 4013 watt all as compared to the rated value of 4000 watt PV. By connecting the PV system to both static and dynamic loads, the PV system can supply power to both loads at rated load powers. However, when subjected to load increase, additional power from the grid is required to supply power to the loads.

## REFERENCES

- [1] T. J. Hammons, J. C. Boyer, S. R. Conners, M. Davies, M. Ellis, M. Fraser, E. A. Holt, and J. Markard, "Renewable energy alternatives for developed countries," *IEEE Transaction on Energy Conversion*, vol. 15, pp. 481-493, December 2000.
- [2] C. Boccaletti, G. Fabbri, J. Marco, E. Santini, "An Overview on Renewable Energy Technologies for Developing Countries: the case of Guinea Bissau," in *International conference on renewable energies and power quality*, Santander, Spain, 2008.
- [3] T. Ryu, "Development of Power Conditioner Using Digital Controls for Generating Solar Power," *Oki Technical Review*, vol. 76, pp. 40-43, 2009.
- [4] J. L. Santos, F. Antunes, A. Chehab And C. C. Cruz, "A Maximum Power Point Tracker For PV Systems Using A High Performance Boost Converter", *Solar Energy*, vol. 80, 2006, pp. 772-778.
- [5] Faranda R., Leva S. and P. L. Vinci, "Energy Comparison of MPPT Techniques for PV Systems", *WSEAS Transaction on Power Systems*, Issue 6, Vol. 3, pp. 446-455, 2008.
- [6] Rong-Jong W., Wen-Hung W., "Grid-Connected Photovoltaic Generation System High", *IEEE Transaction on Circuits and Systems-I: Regular Paper*, Vol. 55, No. 3, April 2008.
- [7] N. S. D'Souza, L. A. C. Lopes, X. Liu, "An Intelligent Maximum Power Point Tracker Using Peak Current Control", *IEEE Power Electronics Specialists Conference*, 2005. PESC '05.
- [8] Hernanz, J.A.R., Martín, J.J.C., Belver, I.Z., Lesaka, J.L., Guerrero, E.Z. & Pérez, E.P. 2010. Modelling of photovoltaic module. *International Conference on Renewable Energies and Power Quality*, pg. 1-5.
- [9] Mohan, N., Undeland, T. M. & Robbins, W. P. 2003. *Power Electronics*. Hoboken: John Wiley & Sons.
- [10] Bouna O. Z., "Contribution to the Study of the Grid Connected Photovoltaic System", Master Thesis, Libya, 2006.

- [11] Sahan B., Vergara A. N., Engler A., Zacharias P., “Development of a Single-Stage Three-Phase PV Module Integrated Converter”, *Power Electronics and Applications*, 2007 European Conference on 2-5 Sept. 2007 Page(s):1 - 11
- [12] Standards-Board, I.S. 2000. *IEEE Recommended Practice for Utility Interface of Photovoltaic (PV) Systems*. New York: The IEEE std 929-2000.